

# Dalton Transactions

Accepted Manuscript



This is an *Accepted Manuscript*, which has been through the Royal Society of Chemistry peer review process and has been accepted for publication.

*Accepted Manuscripts* are published online shortly after acceptance, before technical editing, formatting and proof reading. Using this free service, authors can make their results available to the community, in citable form, before we publish the edited article. We will replace this *Accepted Manuscript* with the edited and formatted *Advance Article* as soon as it is available.

You can find more information about *Accepted Manuscripts* in the [Information for Authors](#).

Please note that technical editing may introduce minor changes to the text and/or graphics, which may alter content. The journal's standard [Terms & Conditions](#) and the [Ethical guidelines](#) still apply. In no event shall the Royal Society of Chemistry be held responsible for any errors or omissions in this *Accepted Manuscript* or any consequences arising from the use of any information it contains.



Journal Name

COMMUNICATION

## Aggregation Induced Phosphorescent *N*-Oxide-2,2'-Bipyridine Bismuth Complexes and Polymorphism-Dependent Emission

Received 00th January 20xx,  
Accepted 00th January 20xx

Oksana Toma,<sup>a</sup> Nicolas Mercier,<sup>\*a</sup> Magali Allain,<sup>a</sup> Alessandra Forni,<sup>\*b</sup> Francesco Meinardi<sup>c</sup> and Chiara Botta<sup>\*d</sup>

DOI: 10.1039/x0xx00000x

www.rsc.org/

**Unprecedented bismuth complexes, based on the rarely used ditopic ligand *N*-oxide-2,2'-bipyridine (*bp2mo*), crystallizing as three polymorphs,  $\alpha$ - (1),  $\beta$ - (2) and  $\gamma$ -[BiBr<sub>3</sub>(*bp2mo*)<sub>2</sub>] (3), exhibit phosphorescence with a Quantum Yield up to 17% for crystal phase (1), while the complex displays a weak fluorescence in solution. A study of the luminescent properties combined with DFT/TDDFT calculations reveals that the lighting phenomenon is originated by aggregation induced phosphorescence correlated to the weak intermolecular interactions present in the different crystal phases.**

While most of the luminogens undergoes a reduction of the emission properties upon aggregation (concentration quenching), some compounds, while non-emissive in solution, become emissive in the solid state. These phenomena are often described as aggregation induced emission (AIE)<sup>1</sup> and, in particular, crystallization induced emission if the emission enhancement occurs only in the crystal and not in the amorphous state.<sup>1b</sup> Since most of the applications in optoelectronics require solid state materials, the interest in compounds showing AIE has shown a very rapid increase. In particular the search of organometallic complexes showing enhanced phosphorescence efficiency in the aggregated state is of high interest. Li and co-workers discovered the aggregation-induced phosphorescence (AIP) phenomenon for the first time in iridium(III) complexes.<sup>2</sup> Thanks to the work of Tang and coworkers the AIE and AIP processes have been rationalized generally in terms of restriction of intramolecular motion (RIM) in aggregated states, which blocks the rotations and vibrations

responsible of the non-radiative pathways in non-rigid environments.<sup>3</sup> To date, organometallic complexes with AIP properties have been reported for several metals, including Ir, Zn, Pd, Pb, Os, Re, Pt.<sup>4</sup> The interest in such materials arises from their possible use in several fields. For example, the assembly and disassembly process of such complexes, able to induce a color change or to switch the emission on and off, can be a powerful tool to obtain dynamic labels for biomedical applications.<sup>5</sup> Indeed, the two often concomitant and opposite effects of concentration quenching and restriction of intramolecular motions make quite difficult to fully control the relationships between structural and emissive properties in these systems.<sup>6</sup> The availability of different polymorphs of a well characterized phosphorescent complex provides the best opportunity to study the relationship between crystal packing and emissive properties.<sup>4f,7</sup>

The oxidized 2,2'-bipyridine derivatives that are the *N*-oxide-2,2'-bipyridine (*bp2mo*) and *N,N'*-dioxide-2,2'-bipyridine (*bp2do*) have been by far less explored than the oxidized 4,4'-bipyridine ligands (*N*-oxide-4,4'-bipyridine (*bp4mo*) and *N,N'*-dioxide-4,4'-bipyridine (*bp4do*))<sup>8-10</sup> in coordination chemistry. To the best of our knowledge, no bismuth complex or coordination polymer based on *bp2mo* has been reported up to now, neither based on *bp2do*, *bp4mo* or *bp4do*. Moreover, we can also notice that complexes with N atoms coordinated to Bi<sup>3+</sup> are not so common. For instance, according to the Cambridge Structural Database<sup>11</sup> only a few structures of Bi-*bp4* complexes are known (*bp4*: 4,4'-bipyridine). Nevertheless, we have recently showed that bipyridine derivatives consisting of one pyridinium cycle (acting as electron acceptor) and one pyridyl (*N*-methyl-4,4'-bipyridinium) or one pyridyl-*N*-oxide part (*N*-*R-N'*-oxide-4,4'-bipyridinium (R= methyl, H)) were able to bind bismuth ions.<sup>12</sup> In this work, we report on three polymorphic complexes in the BiBr<sub>3</sub>/*bp2mo* system:  $\alpha$ - (1),  $\beta$ - (2) and  $\gamma$ -[BiBr<sub>3</sub>(*bp2mo*)<sub>2</sub>] (3). A study of the luminescent properties combined with DFT and Time Dependent DFT calculations and the analysis of the crystal structures show that the phosphorescence in these materials is very sensitive to the environment rigidity, being completely quenched in the solution where only a weak fluorescence signal is detected. We show that the different phosphorescence efficiencies of the three crystal phases are

<sup>a</sup> MOLTECH-Anjou UMR-CNRS 6200, 2 Bd Lavoisier, 49045 Angers, France. Fax: +33 (2) 41 73 54 05; Tel: +33 (2) 41 73 50 83; E-mail: [nicolas.mercier@univ-angers.fr](mailto:nicolas.mercier@univ-angers.fr)

<sup>b</sup> Istituto di Scienze e Tecnologie Molecolari – Consiglio Nazionale delle Ricerche (ISTM-CNR), Università degli Studi di Milano, via C. Golgi 19, 20133 Milano, Italy. [a.forni@istm.cnr.it](mailto:a.forni@istm.cnr.it)

<sup>c</sup> Dipartimento di Scienza dei Materiali, Università degli Studi di Milano Bicocca, via Cozzi 55, I-20125 Milano, Italy.

<sup>d</sup> Istituto per lo Studio delle Macromolecole (ISMAC), CNR, Via Bassini 15, 20133 Milano, Italy. [c.botta@ismac.cnr.it](mailto:c.botta@ismac.cnr.it)

† Footnotes relating to the title and/or authors should appear here.

Electronic Supplementary Information (ESI) available: [Tables of crystal data, X-ray crystallographic files in CIF format and XRPD patterns for 1-3, UV-Vis and PL spectra, PL decays, details of computational results]. See DOI: 10.1039/x0xx00000x

correlated with different non-radiative decay channels induced by their different weak intermolecular interactions.

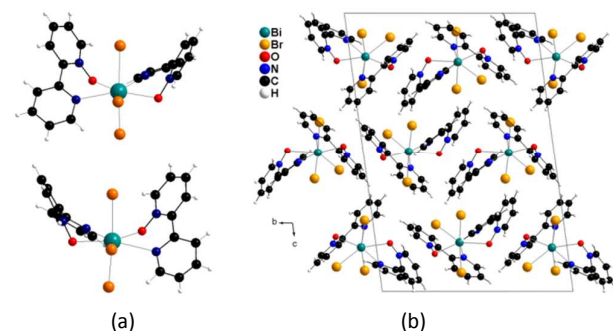


**Fig. 1** (a) The two chiral forms of bismuth complexes found in the structures of  $\alpha$ -,  $\beta$ - and  $\gamma$ -[BiBr<sub>3</sub>(bp2mo)<sub>2</sub>] (**1-3**); (b) crystal structure of **1** viewed along *a*.

All three phases  $\alpha$ -(**1**),  $\beta$ -(**2**),  $\gamma$ -[BiBr<sub>3</sub>(bp2mo)<sub>2</sub>] (**3**) were synthesized by solvothermal method from the mixture of BiBr<sub>3</sub> and bp2mo with acetonitrile as solvent. Slight differences in the stoichiometry of reagents as well as in the temperature program have led to obtain each of the three compounds as pure phases, as checked by XRPD diffraction method (see SI). The X-ray single crystal structures of **1-3** have been refined in the space groups of P-1, P2<sub>1</sub>/n and P2<sub>1</sub>/c, respectively.<sup>†</sup> In all the three structures of **1-3**, a similar neutral complex based on one bismuth ion surrounded by 3 bromides and two bp2mo molecules is found. The geometrical characteristics associated to all these complexes (3 independent complexes in the structure of  $\alpha$ , named **1a**, **1b** and **1c** in the following, and only **1** in the ones of  $\beta$  and  $\gamma$ ) are somewhat different, particularly the dihedral angles between the two cycles of bp2mo molecules and the Bi-N or Bi-O bond distances as well. The two bp2mo molecules are connected to Bi<sup>3+</sup> via their pyridyl and pyridyl-N-Oxide part. The dihedral angle between the two rings (30°-46° range) results from both the N-Bi bond, Bi being in the plane defining by the pyridyl ring, and the (N)O-Bi coordination which involves a N-O-Bi bond angle close to 120° (Fig. 1a). The resulting complex which is completed by three bromides is chiral. But it must be noted that the two chiral forms are present in **1-3** in account of the centrosymmetrical nature of their crystal structure. The overall structures of the three polymorphs differ by the packing of these complex units (the one of **1** is given in Fig. 1b, the ones of **2** and **3** are given in S. I., Fig. S2-S3). The more dense packing is the one of  $\alpha$  (**1**) since the unit cell volume is the smaller ( $2/3V_{\alpha} = 2266 \text{ \AA}^3$ ), then  $\beta$  (**2**) ( $V_{\beta} = 2313 \text{ \AA}^3$ ) and finally  $\gamma$  (**3**) ( $V_{\gamma} = 2367 \text{ \AA}^3$ ). The crystal structures analysis also shows that potential transformations of one phase to another seem difficult.

The experimental absorption spectra of [BiBr<sub>3</sub>(bp2mo)<sub>2</sub>] and the ligand in solution are reported in Figure 2 together with the calculated absorption spectrum of the complex. The lower energy absorption peak of the complex (367 nm) is red-shifted with respect to the ligand (335 nm). Theoretical calculations on the optimized geometries of both ligand and complex allowed to well reproduce the absorption peaks observed in solution. In particular, TD-PBE0/6-311++G(d,p) calculations on the ligand predicted the lowest transition at 324 nm with oscillator strength  $f=0.026$ , while TD-

M062X/def2-SVP calculations on the complex provided the lowest absorption at 369 nm with  $f=0.057$ . This absorption band is principally due to the HOMO→LUMO transition, where HOMO is localized essentially on the inorganic part of the complex and LUMO on the organic ligands (see Figure 3). It is worth noting that such transition, while associated with a significant charge redistribution within the complex, does not imply a charge transfer along a specific direction because the dipole moment is essentially unchanged from the ground (9.75 D) to the excited state (8.05 D). The second peak computed for the complex at 345 nm ( $f=0.015$ , hidden in the convoluted spectrum, see excitation energies in Figure S11a) corresponds principally to the HOMO→LUMO+1 transition, where LUMO+1 is as well localized on the ligands, while the large body of transitions giving the maximum at 274 nm (observed in solution at 270 nm with a shoulder at 295 nm) involve essentially orbitals localized on ligands or bromine atoms.

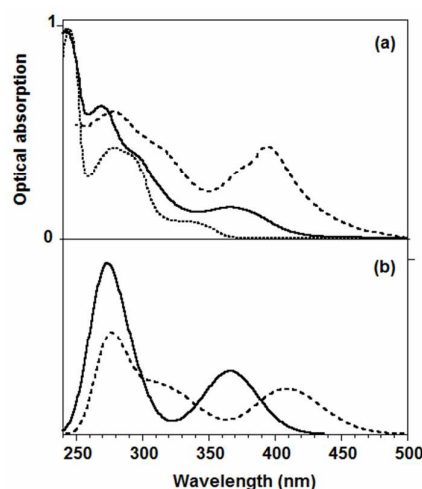


**Fig. 2** (a) Experimental absorption spectra of bp2mo solution (dotted line), [BiBr<sub>3</sub>(bp2mo)<sub>2</sub>] solution (solid line) and  $\alpha$ -[BiBr<sub>3</sub>(bp2mo)<sub>2</sub>] (**1**) solid state (dashed line). (b) Calculated absorption spectrum of [BiBr<sub>3</sub>(bp2mo)<sub>2</sub>] in solution (solid line) and of polymorph **1** (dashed line), obtained by averaging the spectra of **1a**, **1b** and **1c**, resulting from convolution of the excitation energies with 0.2 eV of half-bandwidth

The three polymorphs give rise to essentially the same absorption spectrum (Fig.S7), where the absorption maximum (395, 396 and 392 nm for **1**, **2** and **3**, respectively) is red-shifted with respect to the solution phase (see Fig. 2(a)). TDDFT calculations on the X-ray experimental geometries of **1-3** reproduced as well the red-shift of the absorption maxima with respect to the values obtained at the optimized geometries, with  $\lambda_{\text{max}}$  peaked at 410, 414 and 400 nm for the three molecules of the a.u. of **1**, and at 390 and 410 nm for **2** and **3**, respectively (see Fig. 2b, Fig. S11b-f and Table S2). The two polymorphs **1** and **3** show bright greenish-yellow emissions in the solid state (see Fig. 4, Fig. S7, S8, and Table S1), characterized by different PL efficiency and lifetimes indicative of emission from a triplet state (QY = 17 %,  $\tau = 4.8 \mu\text{s}$ , Commission International d'Éclairage CIE (1931) of (0.34;0.61),  $\lambda_{\text{max}}$  525 nm for **1**; QY = 5 %,  $\tau = 1.0 \mu\text{s}$ ,  $\lambda_{\text{max}}$  503 nm for **3**). Polymorph **2** displays a very weak ( $\lambda_{\text{max}}$  516 nm QY ca. 0.5%) broad emission. On the other hand, the complex [BiBr<sub>3</sub>(bp2mo)<sub>2</sub>] displays an extremely weak emission in

solution (QY=0.01%) with a PL spectrum peaked in the blue region (about 442 nm) characterized by a very short lifetime (258 ps) (see Fig. S9,S10). The different lifetimes and energy position of the emission at the solid state with respect to the solution suggest its origin from a triplet excited state for the former case, and from a singlet excited state for the latter.

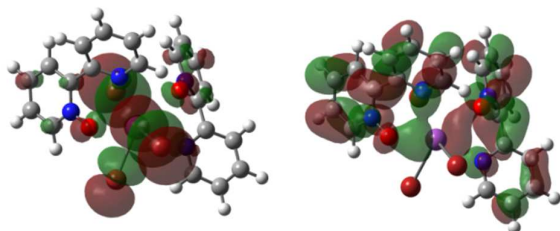


**Fig. 3** Plots of M062X/def2-SVP HOMO (left) and LUMO (right) of the optimized geometry of  $[\text{BiBr}_3(\text{bp}2\text{mo})_2]$  with isosurfaces value 0.02.

To get insight on the nature of the emissive states of the investigated complex, the computed lower energy singlet ( $S_1$ ) and triplet ( $T_1$ ) excited states were submitted to geometry optimization. The obtained stationary states of  $S_1$  and  $T_1$  were quite similar in geometry and the computed emission energies were 669 and 778 nm, respectively. Emission from  $S_1$  could be reasonably associated with the emission peak observed in solution, though placed at lower energy with respect to the experimental one. The observed discrepancy should be ascribed to the intrinsic limitations of the theoretical approach in accurately locating the emissive states when heavy atoms such as bismuth are present. From analysis of the optimized geometries of  $S_1$  and  $T_1$ , it results that one *bp2mo* ligand of the complex underwent a partial planarization with respect to the ground state  $S_0$  geometry (the NCCN torsion angle changes from 44 to 23° and 26° in  $S_1$  and  $T_1$ , respectively), while the other ligand essentially preserves its distortion (the NCCN torsion angle changes from 50 to 47° in both  $S_1$  and  $T_1$ ). The 'planarized' ligand acquires a pseudo-chinoid structure where both the Bi-O and Bi-N bonds significantly strengthen with respect to the  $S_0$  minimum energy geometry (bond lengths go from 2.438, 2.714 in  $S_0$  to 2.237, 2.471 and 2.334, 2.474 Å in  $S_1$  and  $T_1$ , respectively). The  $S_1 \rightarrow S_0$  transition is characterized by an oscillator strength  $f=0.008$  quite lower than the  $S_0 \rightarrow S_1$  one.<sup>13</sup> This finding, coupled with the detected quite fast PL decay time, demonstrates the presence of fast non-radiative decay channels determining the weak PL intensity observed in solution. It is to be noted that at both  $S_1$  and  $T_1$  optimized geometries, the LUMO is localized only on the more planar ligand, while the HOMO essentially preserves its distribution on the inorganic part of the complex (see Fig. S12). Planarization of the ligand, as obtained in the optimized excited states, suggests that the observed emission in solid state is induced by restriction of the torsional motion around the bond connecting the two pyridine moieties.

In order to verify the AIP origin of the emission of the complex in the solid state, we measured the emission of THF frozen solutions of  $[\text{BiBr}_3(\text{bp}2\text{mo})_2]$  (see Fig. 4). Upon solvent solidification the weak blue emission turns into bright greenish-yellow (530 nm), being very similar to the solid state one but showing broader spectral shape, with CIE of (0.39;0.55) (see photos Fig. S13). By heating the

frozen solution, only a reduction in intensity is observed until the melting point of the solvent is reached. Above this temperature the greenish-yellow emission is completely quenched and only the weak deep blue emission, with CIE of (0.15;0.12), is observed (see insert of Fig. 4). Since the sharp quenching of the solution emission occurs exactly at the melting point of the solvent, we assign it to the loss of rigidity of the environment that allows the mobility of the complex ligands. Differently, by rigidification of the solvent matrix of a ligand solution, only minor changes in the emission properties are observed (see Fig. S9). These results demonstrate that the bright phosphorescent emission of the complex crystals can be assigned to their rigidity that prevents intramolecular motions of the ligands. The broadening of the emission band with respect to that observed for **1** and **3** should be ascribed to the amorphous nature of the frozen solution. The different nature of the emissive states (triplet vs singlet) in the rigid environment (solid state and frozen solution) with respect to the solution suggests that the presence of a heavy atom such as Bi induces a fast decay of  $S_1$  via intersystem crossing to the low-lying  $T_1$  triplet. However, the long living phosphorescence of this latter is completely quenched in solution by free intramolecular motions, while the short lived singlet state still preserves in any case a weak fluorescence.

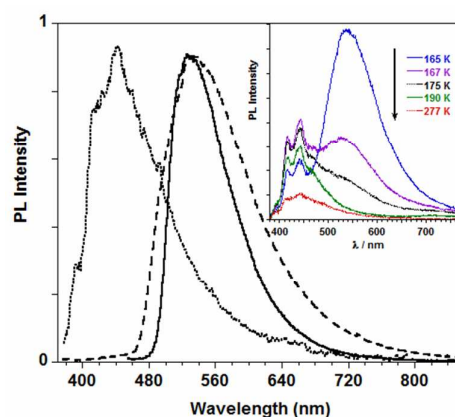


**Fig. 4** Normalized PL spectra of  $[\text{BiBr}_3(\text{bp}2\text{mo})_2]$  THF solutions at room temperature (dotted line) and at 82K (dashed line). PL spectrum of polymorph **1** at room temperature (solid line). Insert: PL spectra of the solution at different temperatures.

Since emission in solid state originates principally from only the  $T_1$  excited state, the stronger emission of polymorph **1** with respect to **2** and, in a lesser extent, **3** should be ascribed to more efficient inhibition of the non-radiative processes connected to intramolecular rotation of the ligands and vibrational relaxation processes. In other words, polymorph **1** seems to possess a higher RIM (Restriction of Intramolecular Motions) property. This interpretation is also confirmed by the observation of the weak emission of films obtained by solution casting. Indeed, as already reported for both organic molecules and complexes, in some cases AIE is not efficient in amorphous films and emission enhancement occurs only in the crystal phase.<sup>3,14,15b</sup> The comparison of these three different crystal polymorphs evidences the important role of the crystal packing in phosphorescent complexes that show crystallization induced phosphorescence. In particular, the different non-radiative decay rates of **1** and **3** (see Table S1) suggest that the



greater QY of **1** is ascribed to its lower rate of non-radiative decay from  $T_1$ . According to previous studies,<sup>15</sup> the non-radiative relaxation can be reduced by the presence of weak intermolecular interactions in the solid state, unlike stronger interactions such as  $\pi$ - $\pi$  stacking which would favour the formation of detrimental excimers. By analyzing the intermolecular interactions network in the crystal structures of **1-3**, we note that only in **1** weak  $\pi$ - $\pi$  interactions are present (see Figure S1), while, in all structures, several C-H $\cdots$ Br, C-H $\cdots$ O and C-H $\cdots$  $\pi$  interactions hold the molecules in their crystalline lattice in a different way (see Table S3). Such hydrogen bonds involve in all cases C-H bonds of one organic ligand and, for C-H $\cdots$ O and C-H $\cdots$  $\pi$  interactions, an acceptor group of another organic ligand, determining an efficient reduction of their conformational flexibility and then of their non-radiative relaxation channel. Moreover, comparing the structures of **1-3**, we observe that, while C-H $\cdots$ Br interactions are similar in the three structures, 'stronger' C-H $\cdots$ O and C-H $\cdots$  $\pi$  hydrogen bonds are found in **1** and **3**, which may explain their higher luminescence with respect to **2**. On the other hand, the higher QY of **1** with respect to **3** could be explained by the lower number of intermolecular interactions found in the latter structure.

In conclusion, we have demonstrated, for the first time for a Bi based complex, that the solid state emission of [BiBr<sub>3</sub>(bp2mo)<sub>2</sub>] complex has an aggregation-induced phosphorescence origin due to restriction of intramolecular motions. We have shown that the phosphorescence efficiency in the solid state is different for the three crystal phases accordingly to their different weak intermolecular interactions. This study highlights the role of even weak intermolecular interactions in the photophysical properties of materials whose phosphorescence is originated by restriction of intramolecular motions.

A. F. acknowledges the MIUR for the PRIN 2010–2011 project no. 2010ERFKXL. C.B. thanks Regione Lombardia for fundings (project "Tecnologie e materiali per l'utilizzo efficiente dell'energia solare" decreto 3667/2013). N. M. thanks the LUMOMAT regional program for a post-doc fellowship to O. T. (Bipylum project).

## Notes and references

† **Crystal data for 1-3** (C<sub>20</sub>H<sub>16</sub>BiBr<sub>3</sub>N<sub>4</sub>O<sub>2</sub>,  $M = 793.08$ ,  $T = 293$  K): **(1)**, triclinic,  $a = 9.6004(4)$  Å,  $b = 15.6899(4)$  Å,  $c = 22.9678(5)$  Å,  $\alpha = 97.53(1)^\circ$ ,  $\beta = 93.73(1)^\circ$ ,  $\gamma = 96.04(1)^\circ$ ,  $V = 3399.8(2)$  Å<sup>3</sup>, space group  $P-1$ ,  $Z = 6$ , crystal size (mm<sup>3</sup>):  $0.20 \times 0.06 \times 0.04$ . **(2)**: monoclinic,  $a = 9.748(1)$  Å,  $b = 13.011(1)$  Å,  $c = 18.253(3)$  Å,  $\beta = 91.88(1)^\circ$ ,  $V = 2313.8(5)$  Å<sup>3</sup>,  $P2_1/n$ ,  $Z = 4$ , crystal size (mm<sup>3</sup>):  $0.11 \times 0.06 \times 0.06$ . **(3)**: monoclinic,  $a = 13.5654(1)$  Å,  $b = 9.6701(1)$  Å,  $c = 18.1116(2)$  Å,  $\beta = 94.96(1)^\circ$ ,  $V = 2367.0(1)$  Å<sup>3</sup>,  $P2_1/n$ ,  $Z = 4$ , crystal size (mm<sup>3</sup>):  $0.29 \times 0.20 \times 0.16$ . The refinements of positions and anisotropic thermal motion parameters of the non-H atoms, converge to  $R_{(F)} = 0.029$  (2471 reflections (11081 collected ( $R_{(int)} = 0.035$ )), 811 parameters),  $wR2_{(F2)} = 0.099$  (all data), GOF on  $F^2$  is 1.17,  $\Delta\rho_{max} = 1.17$  eÅ<sup>-3</sup> for **1**;  $R_{(F)} = 0.071$  (5867 reflections (25911 collected ( $R_{(int)} = 0.010$ )), 271 parameters),  $wR2_{(F2)} = 0.245$  (all data), GOF on  $F^2$  is 1.02,  $\Delta\rho_{max} = 1.403$  eÅ<sup>-3</sup> for **2**, and to  $R_{(F)} = 0.040$  (4865 reflections (10686 collected ( $R_{(int)} = 0.045$ )), 271 parameters),  $wR2_{(F2)} = 0.111$  (all data), GOF on  $F^2$  is 1.08,  $\Delta\rho_{max} = 3.24$  eÅ<sup>-3</sup> for **3**. CCDC 1062361 (**1**), 1062364 (**2**) and 1062365 (**3**).

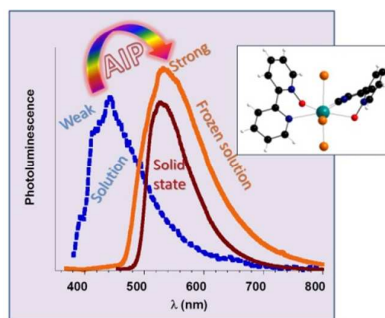
1 (a) J. W. Y. Lam, B. Z. Tang, *Chem. Soc. Rev.*, 2011, **40**, 5361–5388; (b) Y. Dong, J. W. Y. Lam, A. Quin, Z. Li, J. Sun, H.

- H. Y. Sung, I. D. Williams and B. Z. Tang, *Chem. Commun.*, 2007, 40.
- 2 (a) Q. Zhao, L. Li, F.Y. Li, M.X. Yu, Z.P. Liu, T. Yi, C. H. Huang, *Chem. Commun.*, 2008, 685. (b) K. W. Huang, H.Z. Wu, M. Shi, F.Y. Li, T. Yi, C. H. Huang, *Chem. Commun.*, 2009, 1243.
- 3 J. Mei, Y. Hong, J.W.Y. Lam, A. Qin, Y. Tang, B.Z. Tang, *Adv. Mater.* 2014, **26**, 5429–5479.
- 4 (a) G. Li, Y. Wu, G. Shan, W. Che, D. Zhu, B. Song, L. Yan, Z. Su, M.R. Bryce, *Chem. Commun.*, 2014, **50**, 6977. (b) J. Wang, J. Mei, R. Hu, J. Z. Sun, A. Qin, B. Z. Tang, *J. Am. Chem. Soc.*, 2012, **134**, 9956. (c) N.B. Shustova, T.-C. Ong, A. F. Cozzolino, V.K. Michaelis, R.G. Griffin, M. Dinc, *J. Am. Chem. Soc.*, 2012, **134**, 15061. (d) A.J. Qin, J.W.Y. Lam, F. Mahtab, C.K.W. Jim, L. Tang, J.Z. Sun, H.H. Y. Sung, I.D. Williams, B.Z. Tang, *Appl. Phys. Lett.*, 2009, **94**, 253308. (e) J. Shi, N. Chang, C. Li, J. Mei, C. Deng, X. Luo, Z. Liu, Z. Bo, Y.Q. Dong, B. Z. Tang, *Chem. Commun.*, 2012, **48**, 10675. (f) E. Quartapelle Procopio, M. Mauro, M. Panigati, D. Donghi, P. Mercandelli, A. Sironi, G. D'Alfonso, L. De Cola, *J. Am. Chem. Soc.*, 2010, **132**, 14397–14399. (g) S. Liu, H. Sun, Y. Ma, S. Ye, X. Liu, X. Zhou, X. Mou, L. Wang, Q. Zhao, W. Huang, *J. Mater. Chem.*, 2012, **22**, 22167–22173. (h) Y. Chen, L. Qiao, B. Yu, G. Li, C. Liu, L. Ji, H. Chao, *Chem. Commun.*, 2013, **49**, 11095. (i) G.-G. Shan, H.-B. Li, H.-Z. Sun, D.-X. Zhu, H.-T. Cao, Z.-M. Su., *J. Mater. Chem. C*, 2013, **1**, 1440. (j) G.-G. Shan, D.-X. Zhu, H.-B. Li, P. Li, Z.-M. Su, Y. Liao., *Dalton Trans.*, 2011, **40**, 2947.
- 5 M. Mauro, A. Aliprandi, D. Septiadi, N. S. Kehr, L. De Cola, *Chem. Soc. Rev.*, 2014, **43**, 4144.
- 6 Z. Wei, Z.-Y. Gu, R.K. Arvapally, Y.-P. Chen, R.N. Jr. McDougald, J.F. Ivy, A.A. Yakovenko, D. Feng, M.A. Omary, H.-C. Zhou, *J. Am. Chem. Soc.*, 2014, **136**, 8269–8276.
- 7 H. Unesaki, T. Kato, S. Watase, K. Matsukawa, K. Naka, *Inorg. Chem.*, 2014, **53**, 8270–8277.
- 8 (a) A.-C. Chamayou, C. Janiak, *Inorg. Chem. Acta*, 2010, **363**, 2193. (b) S. A. Bourne, L.J. Moitsheki, *J. Chem. Cryst.*, 2007, **37**, 359. (c) J. Jia, A.J. Blake, N. R. Champness, P. Hubberstey, C. Wilson, M. Schröder, *Inorg. Chem.*, 2008, **47**, 8652. (d) H. W. Roesky, M. Andruh, *Coord. Chem. Rev.*, 2003, **236**, 91–119.
- 9 R. J. Hill, D.-L. Long, N. R. Champness, P. Hubberstey, M. Schröder, *Acc. Chem. Res.* 2005, **38**, 337; D.-L. Long, A. J. Blake, N. R. Champness, C. Wilson, M. Schröder, *J. Am. Chem. Soc.* 2001, **123**, 3401; R. J. Hill, D.-L. Long, M. S. Turvey, A. J. Blake, N. R. Champness, P. Hubberstey, C. Wilson, M. Schröder, *Chem. Commun.* 2004, 1792.
- 10 (a) D. J. Hoffart, N. C. Habermehl, S. J. Loeb, *Dalton Trans.*, 2007, 2870. (b) O. Toma, N. Mercier, M. Bouilland, M. Allain, *CrystEngComm*, 2012, **14**, 7844–7847.
- 11 F. H. Allen, *Acta Cryst. Sect. B*, 2002, **58**, 380–388.
- 12 (a) O. Toma, N. Mercier, C. Botta, *Eur. J. Inorg. Chem.*, 2013, 1113–1117. (b) O. Toma, N. Mercier, M. Allain, C. Botta, *CrystEngComm.*, 2013, **15**, 8565.
- 13 TDDFT calculations do not provide information on oscillator strengths for triplet-singlet transitions since spin-orbit coupling effects are not included in current TDDFT implementations.
- 14 (a) E. Cariati, V. Lanzeni, E. Tordin, R. Ugo, C. Botta, A. Giacometti Schieron, A. Sironi and D. Pasini. *Phys. Chem. Chem. Phys.*, 2011, **13**, 18005–18014. (b) Y. Dong, J. W. Y. Lam, A. Qin, J. Sun, J. Liu, Z. Li, J. Sun H. H. Y. Sung, I. D. Williams, H. S. Kwok and B. Z. Tang, *Chem. Commun.*, 2007, 3255.
- 15 (a) H. Tong, Y. Dong, Y. Hong, M. Häussler, J. W. Y. Lam, H. H.-Y. Sung, X. Yu, J. Sun, I. D. Williams, H. S. Kwok, B. Z. Tang, *J. Phys. Chem. C* 2007, **111**, 2287–2294. (b) L. Qian, B. Tong, J. Shen, J. Shi, J. Zhi, Y. Dong, F. Yang, Y. Dong, J. W. Y. Lam, Y. Liu, B. Z. Tang, *J. Phys. Chem. B* 2009, **113**, 9098–9103. (c) Y.

Journal Name

COMMUNICATION

Jin, Y. Xu, Y. Liu, L. Wang, H. Jiang, X. Li, D. Cao, *Dyes Pigments* 2011, **90**, 311-318.



Aggregation Induced Phosphorescence is unprecedentedly observed for a bismuth complex  $[\text{BiBr}_3(\text{bp}2\text{mo})_2]$  ( $\text{bp}2\text{mo} = N\text{-oxide-}2,2'\text{-bipyridine}$ ).